Phase maps of microelectromechanical switches in the presence of the Casimir force and finite plasmon frequency corrections

Palasantzas, G.; De Hosson, J. Th. M.

Published in:
Journal of Applied Physics

DOI:
10.1063/1.2189210

Publication date:
2006

Phase maps of microelectromechanical switches in the presence of the Casimir force and finite plasmon frequency corrections

G. Palasantzas[a] and J. Th. M. DeHosson
Department of Applied Physics, Materials Science Center, University of Groningen, Nijneborgh 4, 9747 AG Groningen, The Netherlands

(Received 31 October 2005; accepted 16 February 2006; published online 24 April 2006)

In this work we explore the influence of self-affine roughness on the phase maps for microelectromechanical switches in the presence of Casimir and electrostatic forces by taking into account finite plasmon frequency corrections for plate separations smaller than the plasmon wavelength λ_P. The phase map depends significantly on the characteristic self-affine roughness parameters (roughness amplitude w, lateral correlation length ξ, and Hurst exponent H) leading to decreasing phase area with increasing roughening at short and/or long roughness wavelengths. The roughness influence is shown to be the prominent factor on phase maps for initial plate separations either smaller or larger than the plasmon wavelength λ_P. © *2006 American Institute of Physics*. [DOI: 10.1063/1.2189210]

I. INTRODUCTION

Microswitches are widely used in the design of micro/nanoelectromechanical system (MEMS/NEMS) applications such as nanotweezers, nanoscale actuators, etc.[1–15] A switch is usually constructed from two conducting electrodes having one usually fixed and the other one moving but suspended by the use of a mechanical spring. By voltage application between the electrodes, the movable electrode moves towards the other electrode because of the electrostatic force. At a certain voltage, the moving electrode becomes unstable and collapses or pulls in to the ground electrode.[3] A two degree of freedom pull-in model was presented in Ref. 4 for a direct calculation of the electrostatic actuators. Residual stress and fringing field effects have also shown to have a great influence on the behavior of rf switches, and strongly influence their failure characteristics.[5,6]

When the proximity between material objects, as, for example, in switches used in MEMS/NEMS, becomes of the order of nanometers up to a few microns, a regime is entered in which forces that are quantum mechanical in nature, namely, van der Waals and Casimir forces become operative.[16] Historically, the Casimir force has been considered to be an exotic quantum phenomenon that results from the perturbation of zero point vacuum fluctuations of the electromagnetic field by the presence of conducting plates.[16–18] The difference in vacuum energy in between and outside the plates leads to the finite Casimir force.[16] The van der Waals forces are operative for separations smaller than ~10 nm, while the Casimir force governs phenomena at separations greater than ~50 nm.[16]

The influence of van der Waals forces on the pull-in voltage between the plates was studied in Ref. 11 by ignoring its influence on the pull-in gap. These studies were extended in Ref. 12 where the effect of the van der Waals force on the pull-in gap was investigated, and an analytical expression of the pull-in gap and voltage was also shown in Ref. 12. The dynamical behavior for nanoscale electrostatic actuators was studied by considering the effect of the van der Waals force in Ref. 13. Furthermore, the influence of the Casimir force on the pull-in gap and voltage, and phase maps of NEMS switches was also studied in Ref. 10 in the limit of perfectly reflecting flat plates coated with Au. An approximate expression of the pull-in gap with the Casimir force was presented by means of perturbation theory including the case of nonlinear electrostatic actuators.[14,15]

Studies of the influence of the Casimir force on the nonlinear behavior of nanoscale electrostatic actuators with flat electrodes showed that their phase maps exhibit periodic orbits around a Hopf point, and a homoclinic orbit to pass through an unstable saddle point.[15] For self-affine rough metal plates[19] it was also shown assuming separations larger than the plasmon wavelength that the fine roughness details at sort and long wavelengths influence stability and the phase maps of microswitches.[20] In many cases the roughness of deposited metal layers, e.g., by sputtering, thermal evaporation, e-beam evaporation, etc., is termed as self-affine, which is characterized by anisotropic scaling of the out of plane dimension with respect to the in plane dimensions.[19]

So far, the former studies for rough plate surfaces[20] were limited to plate separations larger than the plasmon wavelength, while below that length scale finite conductivity effects should strongly be considered in the calculation of the Casimir force by taking simultaneously into account the plate roughness contribution. The finite conductivity correction concerns the fact that real materials with finite conductivity become transparent for electromagnetic waves of frequencies $\omega > \omega_p$, where ω_p is the plasma frequency. Such high frequency modes are not subject to any boundary conditions and therefore their mode density is equal everywhere in space. This phenomenon diminishes the difference in the number of modes inside and outside the volume included between the two bodies and therefore influence the Casimir force. Moreover, the finite conductivity and roughness effect

[a]Author to whom correspondence should be addressed; electronic mail: g.palasantzas@rug.nl

are operating over similar plate separations, and therefore cannot be taken into account in a simple product form.[21] On the other hand, temperature effects are operating at micron plate separations and can be taken into account reasonably well as a multiplication factor for the Casimir force.[21]

II. CONCISE THEORY AND SURFACE ROUGHNESS MODEL

Here, we consider a parallel plate configuration with the electrostatic force and Casimir force pulling the plates together, while an opposing elastic restoring force is present. The initial plate distance is d, the average flat surface area A_f, the plate spring constant k and its mass m, the voltage across the plates V, and ε_o the vacuum permittivity. The restoring and electrostatic forces while not accounting for fringing fields for a plate separation r ($\leqslant d$) are given by[15]

$$F_k = -k(d-r) \text{ and } F_e = \frac{\varepsilon_o A_r}{2}\frac{V^2}{r^2}, \tag{1}$$

where A_r is the surface area of a rough plate surface. For Gaussian height distribution[22] we have a closed expression for the geometric roughness factor R_r so that $A_r = A_f R_r$, which yields for the electrostatic force the expression

$$F_e = \frac{\varepsilon_o A_f}{2}\frac{V^2}{r^2}\int_0^{+\infty} e^{-x}\sqrt{1+\rho_{\rm rms}^2 x}\,dx, \tag{2}$$

where $\rho_{\rm rms} = \sqrt{\langle|\nabla h|^2\rangle}$ is the average local surface slope, which is given after Fourier transformation in the form $\rho_{\rm rms}^2 = \int_0^{Q_c} q^2\langle|h(q)|^2\rangle d^2q/(2\pi)^2$.[23] $Q_c = \pi/a_o$ with a_o an atomic dimension lower roughness cutoff.

Furthermore, assuming single valued roughness fluctuations $h(R)$ of the in-plane position $R=(x,y)$ and the same roughness for both plates, the Casimir energy is given by[21]

$$E_{\rm Cr} = E_{\rm Cf} + \frac{1}{2}\left(\frac{\partial^2 E_{\rm Cf}}{\partial r^2}\right)\left[2\int P(q)\langle|h(q)|^2\rangle\frac{d^2q}{(2\pi)^2}\right], \tag{3}$$

with $E_{\rm Cf} = -(\pi^2\hbar c/720r^3)A_f$ the Casimir energy for flat perfectly conducting plates, and $\langle|h(q)|^2\rangle$ the roughness spectra ($\langle h\rangle = 0$). The scattering function $P(q)$ and taking into account the fact that metals have a finite plasmon wavelength λ_P (e.g., $\lambda_P \approx 100$ nm for Al, 130 nm for Au, etc.), it is given by the simplified expressions[21]

$$P(p) = \begin{cases} \text{if } d < \lambda_P\text{:} & 0.4492dq \quad \text{for } q \gg 2\pi/d, \quad q \gg 2\pi/\lambda_P \\ \text{if } d > \lambda_P\text{:} & \begin{cases} (1/3)dq & \text{for } 2\pi/d \ll q \ll 2\pi/\lambda_P \\ (7\lambda_P/15\pi)q & \text{for } q \gg 2\pi/d, \quad q \gg 2\pi/\lambda_P. \end{cases} \end{cases} \tag{4}$$

Equation (4) is derived assuming that the optical response of the metallic plates is described by a plasma model with a dielectric function $\varepsilon(\omega) = 1-(\omega_p/\omega)^2$, where ω_P is the plasma frequency. Upon substitution of Eq. (4) into Eq. (3) we obtain for the Casimir force,

$$F_{\rm Cr} = -\frac{dE_{\rm Cr}}{dr} \cong F_{\rm Cf}\left(1+\frac{2C_r}{r}\right), \tag{5}$$

$$C_r = \begin{cases} 0.4492\displaystyle\int_{Q_d}^{Q_c} q\langle|h(q)|^2\rangle\frac{d^2q}{(2\pi)^2} & \text{if } d < \lambda_P \\ \dfrac{1}{3}\displaystyle\int_{Q_d}^{Q_{\lambda_P}} q\langle|h(q)|^2\rangle\frac{d^2q}{(2\pi)^2} + \frac{7}{15\pi}\frac{\lambda_P}{d}\int_{Q_{\lambda_P}}^{Q_c} q\langle|h(q)|^2\rangle\frac{d^2q}{(2\pi)^2} & \text{if } d > \lambda_P, \end{cases} \tag{6}$$

where $Q_{\lambda_P} = 2\pi/\lambda_P$ and $Q_d = 2\pi/d_y$. Finally, if we consider the change of variables so that $u = r/d$, $M = m/kT^2$, $\tau = t/T$ (T a characteristic time), $\alpha = \pi^2\hbar A_f/kd^5$, and $\beta = \varepsilon_o A_f V^2/kd^3$,[15] the second law of Newton $m(d^2r/dt^2) = |F_k| - |F|_e - |F_{\rm Cr}|$ that describes the plate motion takes the more convenient form

$$M\frac{d^2u}{d\tau^2} = 1 - u - \frac{\beta R_r}{2u^2} - \frac{\alpha}{240u^4}\left(1+\frac{2C_r}{du}\right), \tag{7}$$

where any meaningful solution must satisfy the condition $0 < u < 1$.

From Eqs. (6) and (7) further calculations require evaluation of the roughness factor C_r. A wide variety of surfaces and interfaces that appear in thin films grown under nonequilibrium conditions posseses the so-called self-affine roughness.[19] In this case the roughness spectrum $\langle|h(q)|^2\rangle$ shows a power law scaling.[19] $\langle|h(q)|^2\rangle \propto q^{-2-2H}$ if $q\xi \gg 1$ and $\langle|h(q)|^2\rangle \propto$ const if $q\xi \ll 1$. This is satisfied by the analytical description,[23]

$$\langle|h(q)|^2\rangle = 2\pi\frac{w^2\xi^2}{(1+aq^2\xi^2)^{1+H}}, \tag{8}$$

with $a = 1/2H[1-(1+aQ_c^2\xi^2)^{-H}]$ $(0 < H < 1)$, and $a = 1/2\ln(1+aQ_c^2\xi^2)$ $(H=0)$. Small values of the roughness or

Hurst exponent H (~ 0) characterize jagged or irregular surfaces; while large values H (~ 1) surface with smooth hills and valleys.[19] For other correlation models see also Refs. 19 and 24.

III. RESULTS AND DISCUSSION

The electrostatic term in Eq. (2) can take an analytical expression in the weak roughness limit ($\rho_{\rm rms} < 1$) where the present analysis applies. Expansion of the integral in Eq. (2) yields the series expansion,

$$F_e \cong \frac{\varepsilon_o A_f}{2}\frac{V^2}{r^2}\left[1+\frac{1}{2}\rho_{\rm rms}^2+\sum_{n=2}^{+\infty} S(n)\rho_{\rm rms}^{2n}\right], \tag{9}$$

with $S(n)=[1\cdot 1\cdot 3\cdot 5\cdots(2n-3)](-1)^{n-1}/2^n$. In terms of Eq. (8) we have for the average local surface slope $\rho_{\rm rms}$ the analytic form $\rho_{\rm rms}^2=(w^2/2\xi^2 a^2)\{(1-H)^{-1}[(1+aQ_c^2\xi^2)^{1-H}-1]-2a\}$, which gives an analytic form for the electrostatic force in a form of series.

On the other hand, the roughness correction to the Casimir force in Eqs. (5) and (6) can be calculated analytically for the three characteristic roughness exponents $H=0$, 0.5, and 1. Thus, we have

$$C_r^{H=0}=w^2\begin{cases}0.4492\left\{\dfrac{1}{a}(Q_c-Q_d)-\dfrac{1}{a^{3/2}\xi}[\tan^{-1}(u)|_{X_d}^{X_c}]\right\} & \text{if } d<\lambda_P\\ \dfrac{1}{3}\left\{\dfrac{1}{a}(Q_{\lambda_P}-Q_d)-\dfrac{1}{a^{3/2}\xi}[\tan^{-1}(u)|_{X_d}^{X_{\lambda_P}}]\right\}+\dfrac{7}{15\pi}\dfrac{\lambda_P}{d}\left\{\dfrac{1}{a}(Q_c-Q_{\lambda_P})-\dfrac{1}{a^{3/2}\xi}[\tan^{-1}(u)|_{X_{\lambda_P}}^{X_c}]\right\} & \text{if } d>\lambda_P,\end{cases} \tag{10}$$

$$C_r^{H=0.5}=w^2\begin{cases}0.4492\left\{\dfrac{1}{a^{3/2}\xi}[\sinh^{-1}(u)|_{X_d}^{X_c}]-\dfrac{1}{a}[Q_cT_c^{-1/2}-Q_dT_d^{-1/2}]\right\} & \text{if } d<\lambda_P\\ \dfrac{1}{3}\left\{\dfrac{1}{a^{3/2}\xi}[\sinh^{-1}(u)|_{X_d}^{X_{\lambda_P}}]-\dfrac{1}{a}[Q_{\lambda_P}T_{\lambda_P}^{-1/2}-Q_dT_d^{-1/2}]\right\}+\dfrac{7}{15\pi}\dfrac{\lambda_P}{d}\left\{\dfrac{1}{a^{3/2}\xi}[\sinh^{-1}(u)|_{X_{\lambda_P}}^{X_c}]-\dfrac{1}{a}[Q_cT_c^{-1/2}-Q_{\lambda_P}T_{\lambda_P}^{-1/2}]\right\} & \text{if } d>\lambda_P,\end{cases} \tag{11}$$

$$C_r^{H=1}=w^2\begin{cases}0.4492\left\{\dfrac{1}{a^{3/2}\xi}[\tan^{-1}(u)|_{X_d}^{X_c}]-\dfrac{1}{2a}[Q_cT_c^{-1}-Q_dT_d^{-1}]\right\} & \text{if } d<\lambda_P\\ \dfrac{1}{3}\left\{\dfrac{1}{a^{3/2}\xi}[\tan^{-1}(u)|_{X_d}^{X_{\lambda_P}}]-\dfrac{1}{2a}[Q_{\lambda_P}T_{\lambda_P}^{-1}-Q_dT_d^{-1}]\right\}+\dfrac{7}{15\pi}\dfrac{\lambda_P}{d}\left\{\dfrac{1}{a^{3/2}\xi}[\tan^{-1}(u)|_{X_{\lambda_P}}^{X_c}]-\dfrac{1}{2a}[Q_cT_c^{-1}-Q_{\lambda_P}T_{\lambda_P}^{-1}]\right\} & \text{if } d>\lambda_P,\end{cases} \tag{12}$$

with $L(x)|_A^B=L(B)-L(A)$, $X_c=\sqrt{a}\xi Q_c$, $X_d=\sqrt{a}\xi Q_d$, $X_{\lambda_P}=\sqrt{a}\xi Q_{\lambda_P}$, $T_c=1+(X_c)^2$, $T_{\lambda_P}=1+(X_{\lambda_P})^2$, and $T_d=1+(X_d)^2$. We should note that we consider for the scattering function $P(q)$ the power law regimes from which deviations occur for wave vectors $q<10^{-3}$ where $P(q)\ll 1$.[20] On the other hand, the roughness spectrum approaches the asymptotic limit $\langle|h(q)|^2\rangle\approx(2\pi)w^2\xi^2$ for $q\xi\ll 1$, minimizing the error by considering only the power law approximation.

Furthermore, the calculations of the phase maps were performed with $a_o=0.3$ nm, plasmon wavelength $\lambda_P=100$ nm, effective system mass $M=1$, and initial conditions $u=0.67$ and $du/d\tau=0$ (at $\tau=0$). Figure 1 shows calculations of phase maps, $du/d\tau$ vs u for two consecutive roughness exponents H and various separations respectively, $d=80$, 120, 200 nm, below and above the plasmon wavelength λ_P. With decreasing roughness exponent H (or for a roughened surface at short wavelengths) the phase map area is decreasing in a rather sensitive manner even for exponents very close in value. It is evident that the roughness exponent influence has the most significant influence for initial plate separations either larger or smaller than λ_P. As the inset of Fig. 1 shows with increasing plate separation the phase area increases, however, at a lower rate for separations larger than λ_P.

If we compare with the influence of the lateral roughness correlation length ξ in Fig. 2 and the roughness amplitude w as shown in Fig. 3, it becomes clear that also these long wavelength roughness parameters give a predominant influence, whereas the influence of the initial plate separation d on the phase maps is negligibly small. This is because the plate separation enters through the influence of the roughness term which in turn becomes weaker by decreasing roughness amplitude w and/or increasing roughness exponent H and correlation length ξ. Therefore, it becomes clear from comparison of Figs. 1–3 that increasing surface roughening at short and/or long wavelengths leads to predominant effects on the phase maps rather than the initial plate separation. This is also manifested by plotting (Fig. 4) the influence, for example, of the roughness H on the phase speed $du/d\tau$ and the normalized displacement u versus normalized time $\tau(=t/T)$. Notably for both quantities ($du/d\tau$ and u) the influence of the roughness exponent H is rather evident and increases fast with decreasing roughness exponent H or equivalently with increasing plate surface roughness.

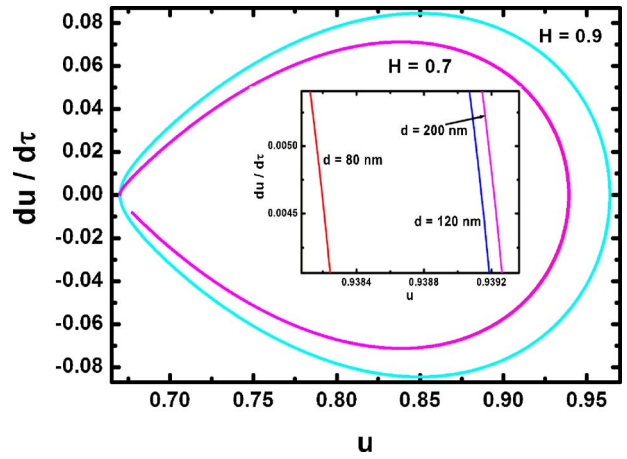

FIG. 1. (Color online) Calculation of phase maps $du/d\tau$ vs u for a_o =0.3 nm, M=1, λ_P=100 nm, w=5 nm, ξ=200 nm, a=10, β=0.1, two consecutive values of the roughness exponent H=0.7 and H=0.9, and plate separations d=80, 120, 200 nm. The inset shows more clear the influence of the plate separation d for H=0.7.

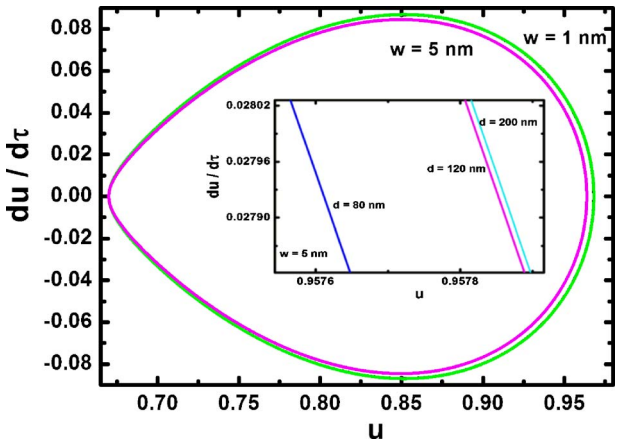

FIG. 3. (Color online) Calculation of phase maps $du/d\tau$ vs u for a_o =0.3 nm, M=1, λ_P=100 nm, ξ=200 nm, a=10, β=0.1, H=0.7, for amplitudes w as indicated, and plate separations d=80, 120, 200 nm. The inset shows for w=5 nm the weak dependence on d.

Finally, we should mention that the Casimir force and energy depend on the dielectric properties of the materials in a complicated manner.[25] Thin films, which are used to coat plates of switches, are described with spatially dispersive nonlocal dielectric functions. It has been shown that even for film thickness smaller than the electron mean free path, the difference between the local and nonlocal calculations of the Casimir force is of the order of a few tenths of a percent. Thus the local description of thin metallic films where the optical response depends only on frequency is adequate within the current experimental precision and range of separations.[25] By restricting ourselves to the influence of roughness, the assumption of the plasmon model is a reasonable one (e.g., for Al layers).

IV. CONCLUSIONS

In summary, we have investigated the influence of self-affine roughness on the phase maps for microelectromechanical switches in the presence of Casimir and electrostatic forces by taking into account the finite plasmon frequency corrections for plate separations smaller than the plasmon wavelength λ_P. The plate medium was described by the local plasmon dielectric function of free electrons ignoring any nonlocal effects. In this case it is shown that the phase map depends significantly on the characteristic self-affine roughness parameters (roughness amplitude w, lateral correlation length ξ, and Hurst exponent H) leading to decreasing phase area with increasing roughening at short and/or long roughness wavelengths. The roughness influence is shown to be

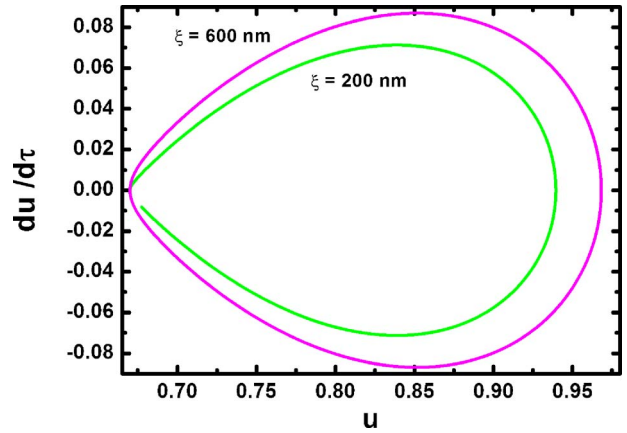

FIG. 2. (Color online) Calculation of phase maps $du/d\tau$ vs u for a_o =0.3 nm, M=1, λ_P=100 nm, w=5 nm, a=10, β=0.1, H=0.7, two different correlation lengths as indicated, and plate separations d=80, 120, 200 nm.

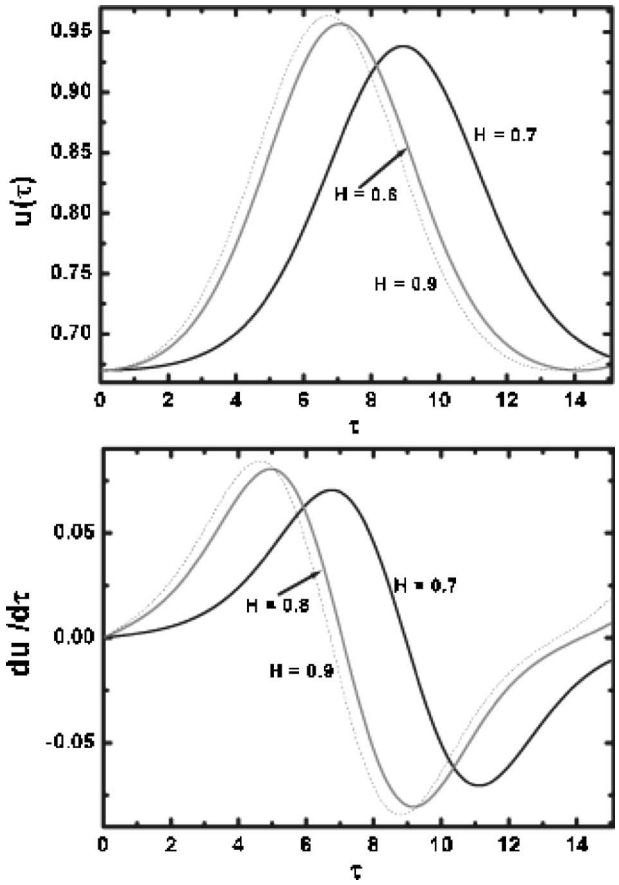

FIG. 4. (Color online) Calculation of $du/d\tau$ and $u(\tau)$ vs $\tau(=t/T)$ for a_o =0.3 nm, M=1, λ_P=100 nm, w=5 nm, ξ=200 nm, a=10, β=0.1, roughness exponents H as indicated, and plate separation d=50 nm.

the most prominent factor on phase maps for initial plate separations either smaller or larger than the plasmon wavelength λ_P. This study shows that proper surface roughness measurements are necessary to characterize the morphology (e.g., by x-ray scattering techniques, electron diffraction, scanning probe microscopy,[19,23,24] etc.) at all relevant roughness wavelengths in order to gauge properly its influence on the Casimir and electrostatic forces and further on device operation.

ACKNOWLEDGMENT

We would like to thank Dr. D. Iannuzzi for useful discussions on the Casimir effect and finite conductivity effects.

[1]P. Kim and C. M. Lieber, Science **286**, 2148 (1999).
[2]S. Akita, Y. Nakayama, S. Mizooka, Y. Takano, T. Okawa, Y. Miyatake, S. Yamanaka, M. Tsuji, and T. Nosaka, Appl. Phys. Lett. **79**, 1691 (2001).
[3]P. M. Osterberg, Ph.D. dissertation, MIT, 1995.
[4]O. Bochobza-Degani and Y. Nemirovsky, Sens. Actuators, A **97–98**, 569 (2002).
[5]O. Bochobza-Degani, E. Socher, and Y. Nemirovsky, Sens. Actuators, A **97**, 563 (2002).
[6]L. X. Zhang, J. W. Zhang, Y.-P. Zhao, and T. X. Yu, Int. J. Nonlinear Sci. Numer. Simul. **3**, 353 (2002).
[7]L. X. Zhang and Y.-P. Zhao, Microsyst. Technol. **9**, 420 (2003).
[8]L. J. Hornbeck, U.S. Patent No. 5,061,049 1991.
[9]J. A. Pelesko, Proceedings of Modeling Simulation Microsystems, 2001, Hilton Head, S.C. (Nanotech, 2001), Vol. 1, p. 290–293, ISBN: 0-9708275-0-4.
[10]E. Buks and M. L. Roukes, Europhys. Lett. **54**, 220 (2001).
[11]M. Dequesnes, S. V. Rotkin, and N. R. Aluru, Nanotechnology **13**, 120 (2002).
[12]S. V. Rotkin, Proc.-Electrochem. Soc. 6, 90 (2002).
[13]W. H. Lin and Y.-P. Zhao, Chin. Phys. Lett. **20**, 2070 (2003).
[14]R. Seydel, *Practical Bifurcation and Stability Analysis: From Equilibrium to Chaos*, Interdisciplinary Applied Mathematics Vol. 5, 2nd ed. (Springer-Verlag, New York, 1994).
[15]W. H. Lin and Y.-P. Zhao, Chaos, Solitons Fractals **23**, 1777 (2005); Microsyst. Technol. **11**, 80 (2005). For the electrostatic force between flat plates see also P. M. Osterberg, Ph.D. dissertation, MIT, 1995.
[16]H. B. G. Casimir, Proc. K. Ned. Akad. Wet. **51**, 793 (1948).
[17]J. N. Israelachvili, *Intermolecular and Surface Forces* (Academic, London, 1992).
[18]M. Kardar and R. Golestanian, Rev. Mod. Phys. **71**, 1233 (1999).
[19]P. Meakin, Phys. Rep. **235**, 1991 (1994); J. Krim and G. Palasantzas, Int. J. Mod. Phys. B **9**, 599 (1995); Y.-P. Zhao, G.-C. Wang, and T.-M. Lu, *Characterization of Amorphous and Crystalline Rough Surfaces-Principles and Applications*, Experimental Methods in the Physical Science, Vol. 37 (Academic, New York, 2001).
[20]G. Palasantzas and J. Th. M. DeHosson, Phys. Rev. B **72**, 121409 (2005); Phys. Rev. B **72**, 115426 (2005).
[21]P. A. Maia Neto, A. Lambrecht, and S. Reynaud, Phys. Rev. A **72**, 012115 (2005); Europhys. Lett. **69**, 924 (2005); C. Genet, A. Lambrecht, P. Maia Neto, and S. Reynaud, *ibid.* **62**, 484 (2003); T. Emig, A. Hanke, R. Golestanian, and M. Kardar, Phys. Rev. Lett. **87**, 260402 (2001); G. Palasantzas, J. Appl. Phys. **97**, 126104 (2005).
[22]B. N. J. Persson and E. J. Tosatti, J. Chem. Phys. **115**, 5597 (2001).
[23]G. Palasantzas, Phys. Rev. E **56**, 1254 (1997); Phys. Rev. B **48**, 14472 (1993); **49**, 5785 (1994).
[24]S. K. Sinha, E. B. Sirota, S. Garoff, and H. B. Stanley, Phys. Rev. B **38**, 2297 (1988); H. N. Yang and T. M. Lu, *ibid.* **51**, 2479 (1995); Y. P. Zhao, G. C. Wang, and T. M. Lu, *ibid.* **55**, 13938 (1997).
[25]R. Esquivel-Sirvent and V. B. Svetovoy, Phys. Rev. B **72**, 045443 (2005).